Initial result on iron transport analysis using radial profiles measured by space-resolved EUV spectrometer in LHD

X. L. HUANG[1], S. Morita[1,2], T. Oishi[1,2], M. Goto[1,2], H. M. Zhang[1], I. Murakami[1,2]

[1] *Department of Fusion Science, Graduate University for Advanced Studies, Toki 509-5292, Gifu, Japan*

[2] *National Institute for Fusion Science, Toki 509-5292, Gifu, Japan*

Abstract

The Fe n=3-2 transition array consisting of Fe^{16+} through Fe^{23+} ions is utilized for impurity transport study in the Large Helical Device (LHD). Since the charge states of Fe^{16+} through Fe^{23+} are usually distributed all over the whole volume of LHD plasmas, the impurity transport can be studied without any assumption on the radial structure of transport coefficients. A one-dimensional transport code is employed to simulate the emissivity profile of iron line emissions. The transport coefficient is then determined by fitting the experimental profile of n=3-2 Fe transitions in several ionization stages with the impurity transport code. A preliminary result of the iron transport analysis in high and low electron density discharges is reported.

I. Introduction

Radial transport of impurity ions remains as an important issue in magnetically confined fusion devices, since the plasma performance is significantly affected by radiation loss and fuel dilution caused by impurities. In the Large Helical Device (LHD), the density profile can exhibit a peaked, flat or hollow shape, depending on plasma conditions such as B_t, T_e, and n_e. Therefore, it is of great importance to investigate corresponding impurity transport in the plasma core of LHD[1-4]. With a centrally peaked density profile in high-density LHD discharges, impurity accumulation has been clearly observed and the transport is analyzed based on an assumption of the radial structure of convective velocity[5]. Nevertheless, analysis on the detail structure of transport coefficients is still necessary for better understanding of the radial transport. Formation of the hollow or flat density profile observed in the LHD is quite unique in tokamaks. Therefore, the LHD plasma can give a good opportunity for studying the impurity transport through the analysis of radial structure in the transport coefficient, in particular in relation to the density and temperature gradients.

Iron is an intrinsic impurity in magnetically confined fusion plasmas and therefore is useful for comprehensive study of the impurity transport under different plasma conditions. For the purpose, the Fe n=3-2 Lα transition array, emitted in narrow wavelength range of 10 – 18 Å, is of great advantage because the transition array includes emissions from ions in several charge states of Fe^{16+} through Fe^{23+}. In addition, these iron emissions have relatively strong emissivities and are distributed all over the whole plasma volume of the LHD as the ionization energy of corresponding ions stays between 1 keV and 2 keV of which the range is nearly equal to electron temperature in core plasmas of the LHD. Radial profiles of the Fe Lα emissions have been well measured by a space-resolved extreme-ultraviolet (EUV) spectrometer[6]. It is then possible to determine the transport coefficient, i.e. the diffusion coefficient and the convective velocity, from the emissivity profile with the help of impurity transport simulation. It should be noted that the iron transport can be analyzed along the minor radius without any assumption on the radial structure of transport coefficients because the Fe Lα transition with several ionization stages is emitted over wide range of the radial plasma location.

II. Experimental setup and Fe n=3-2 array

The EUV system used for this study is working in the wavelength range of 10-130Å, mainly consisting of an entrance slit, a spatial-resolution slit, a gold-coated concave varied-line-spacing (VLS) laminar-type holographic grating with a groove density of 2400 per mm and a charge-coupled device (CCD) detector with 1024 × 255 pixels, as shown in Fig. 1(a). A relatively long distance between the spectrometer and the plasma is necessary for observing the vertical plasma range of 50 cm. In practice the distance between the central plasma position and the entrance slit of the spectrometer is set to 9157 mm when the plasma axis position is R = 3.90 m. Since the distance between the entrance slit and the CCD detector is roughly 470 mm, which is a weak function of wavelength, we obtain a multiplication factor of 19.5. The EUV spectrometer is installed on a mid-plane port at the backside of rectangular vacuum extension chamber.

The elevation angle of the central viewing chord is exactly determined to make possible the profile measurement at upper half vertical range of the elliptical plasma, i.e., Z = 0–50 cm. Figure 1(b) shows top view of the optical layout in the spectrometer. EUV radiation emitted from LHD plasmas passes through the entrance slit and reaches the grating adjusted at the angle of incidence of 88.6°. The radiation diffracted on the grating is focused on the focal plane and recorded by the CCD detector. The large angle of incidence is necessary for observing the EUV light in such a short wavelength range with high throughput.

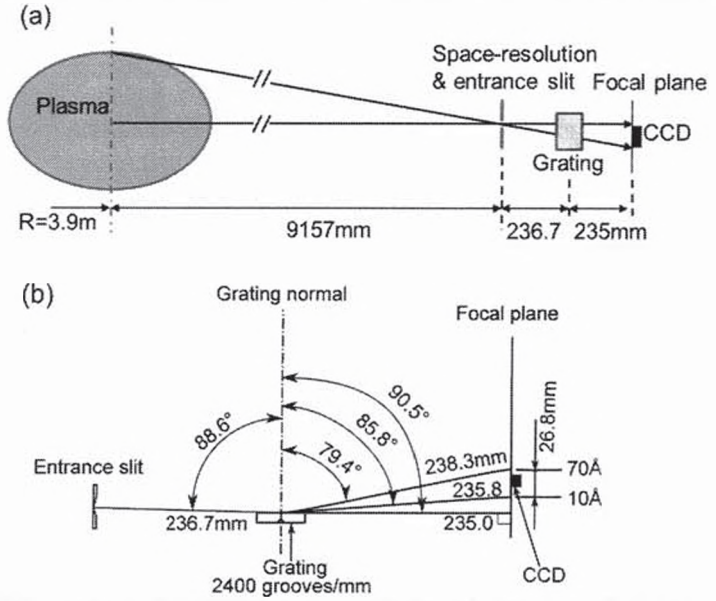

FIG. 1. Schematics of (a) EUV system and (b) optical layout of the spectrometer.

Iron spectrum with n = 3-2 Lα transitions between 10 and 20 Å has been measured by injecting an iron impurity pellet[7]. A typical result is shown in Fig. 2. A lot of Lα transitions from highly ionized iron ions are observed in the spectrum. Since many iron lines are blended, the spectrum appears with structure like pseudo-continuum. The line-integrated vertical profile of the Fe Lα transition from FeXVII to FeXXIV is analyzed by carefully choosing the wavelength interval at each ionization stage. The result is shown in Fig. 3(a). The electron density and temperature profiles are also shown in Fig. 3(b) of which the coordinate is converted into the vertical position at horizontally elongated plasma cross section by taking into account the elliptical magnetic surface. The vertical profile is normalized at each peak position. The peak position of each profile moves inside with increase in the ionization stage, reflecting the centrally peaked electron temperature profile.

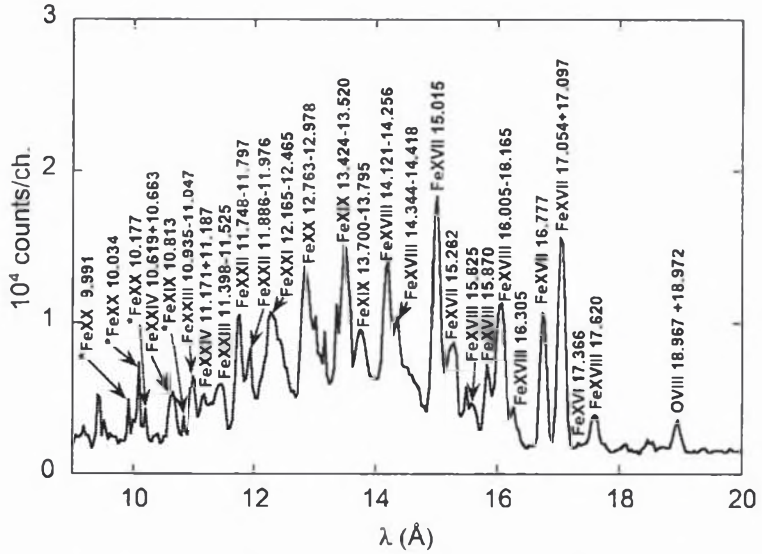

FIG. 2. Fe n = 3–2 Lα spectrum below 20 Å measured after iron impurity pellet injection in NBI discharge with central electron temperature of 3keV. The asterisks (*) before wavelengths denote that two or more lines are blended into the same wavelength position.

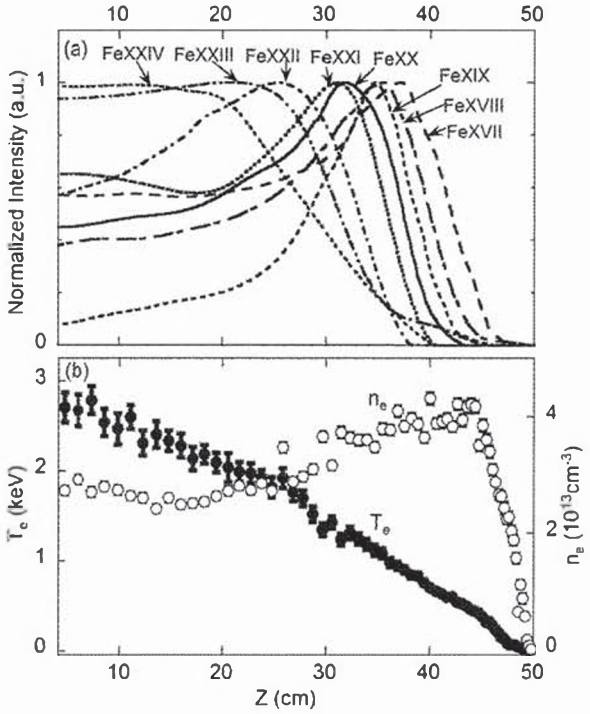

FIG. 3. (a) Line-integrated vertical intensity profiles of FeXVII (17.054 Å + 17.097 Å), FeXVIII (14.121–14.256 Å), FeXIX (13.424–13.520 Å), FeXX (12.763–12.978 Å), FeXXI (12.165–12.465 Å), FeXXII (11.748–11.797 Å), FeXXIII (10.935–11.047 Å), and FeXXIV (10.619 Å + 10.663 Å) and (b) electron temperature (closed circles) and density (open circles) profiles.

Experimental emissivity profiles can be derived from the vertical profile in Fig.3 (a) based on an Abel inversion technique. The magnetic surface structure in LHD plasmas is calculated with variation moment equilibrium code (VMEC)[8,9]. Then, the chord length between adjacent magnetic surfaces along the observation chord of the spectrometer is evaluated at all magnetic surfaces taking into account the finite-β effect. Here, it should be pointed out that the magnetic flux surface is also assumed outside the last close flux surface (LCFS) by extrapolating the magnetic surface contour. Although the assumption may cause certain uncertainty, it does not strongly affect the emissivity peak inside the LCFS because the emissivity outside the LCFS is usually weak.

III. Transport simulation

A one-dimensional impurity transport code is employed to determine the transport coefficient[10,11]. It is assumed that the impurity transport satisfies the following equation:

$$\Gamma_q = -D_q(r)\frac{\partial n_q}{\partial r} + V_q(r)n_q, \quad (1)$$

where Γ_q, n_q, D_q, V_q are the particle flux, the ion density, the diffusion coefficient and the convective velocity of impurity ions in the qth charge state, respectively. Positive and negative velocities stand for outward and inward convection, respectively.

With given transport coefficients and radial profiles of plasma parameters, the code calculates the impurity ion density in all charge states as a function of time. The impurity source is assumed to originate in the sputtering at the first wall of vacuum vessel. In this study, the iron ion density profile in a steady state is used for analysis. The ergodic layer of LHD plasma is not considered in the present work. Consequently, a slight error may occur near the last close flux surface (LCFS) in the simulated result. Nevertheless, the error is usually negligibly small.

The transport coefficient near the emissivity peak can be determined by comparing the emissivity profile obtained from experiment and simulation. In order to determine the transport coefficient at the whole plasma volume, the iron emission is simultaneously analyzed at several charge states. The emissivity profile is calculated from the simulated ion density profile based on intensity coefficients obtained with the HULLAC code[12] and compared with the experimental emissivity profile, which is calculated from the measured line-integrated profile as mentioned in Section II.

IV. Transport analysis at low- and high-density discharges

Impurity accumulation has been observed with a centrally peaked density profile after hydrogen multi-pellet injection in the LHD5. Here, the radial structure of the transport coefficient is analyzed using emissions of FeXVII at 15.02Å and FeXVIII at 14.20Å. The waveform of a high-density discharge with multiple H_2 pellets is shown in Fig. 4 for the line-averaged electron density (n_e), central electron temperature ($T_e(0)$), total radiation power (P_{rad}) and plasma stored energy (W_p) together with NBI port-through power (P_{NBI}). The emission profile is measured at the time frame denoted with hatched area (t=4.6-4.8s) in Fig. 4, at which the plasma stays in a quasi-steady state. The experimental and simulated emissivity profiles are plotted in Figs. 5(a) and (b), respectively. The coefficients determined from the comparison of two emissivity profiles are shown in Fig. 5(c). Figure 5(d) displays corresponding electron temperature and density profiles measured by Thomson scattering system. The simulated emissivity profile is basically in a good agreement with experimental one. The diffusion coefficient, D, is constant along the minor radius, while the convective velocity, V, increases as an inward convection toward plasma outer region and then keeps constant in the plasma periphery ($0.75 \leq \rho \leq 1$). When comparing Fig. 5(c) with (d), the structure of V seems to change with the density profile. The shape of V roughly agrees with conventionally assumed shape, e.g. V is proportional to the normalized minor radius.

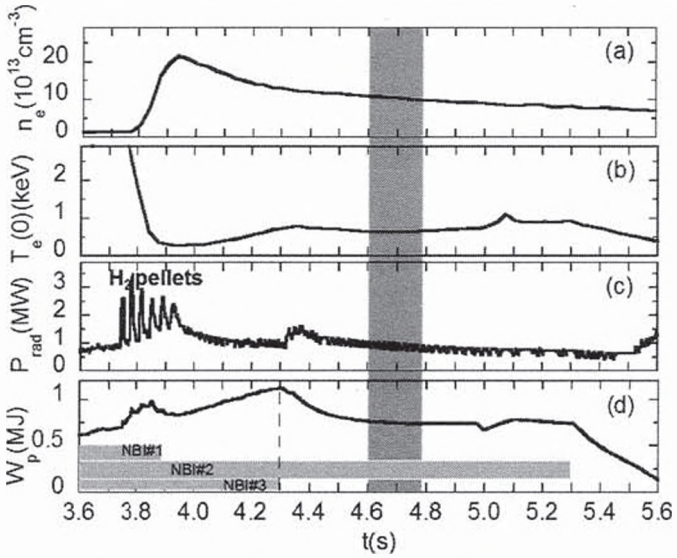

FIG. 4. Time evolution of (a) line-averaged electron density, (b) central electron temperature, (c) radiation power, and (d) plasma stored energy together with NBI port-through power. The vertical hatched region denotes the time frame when the emission profile is measured.

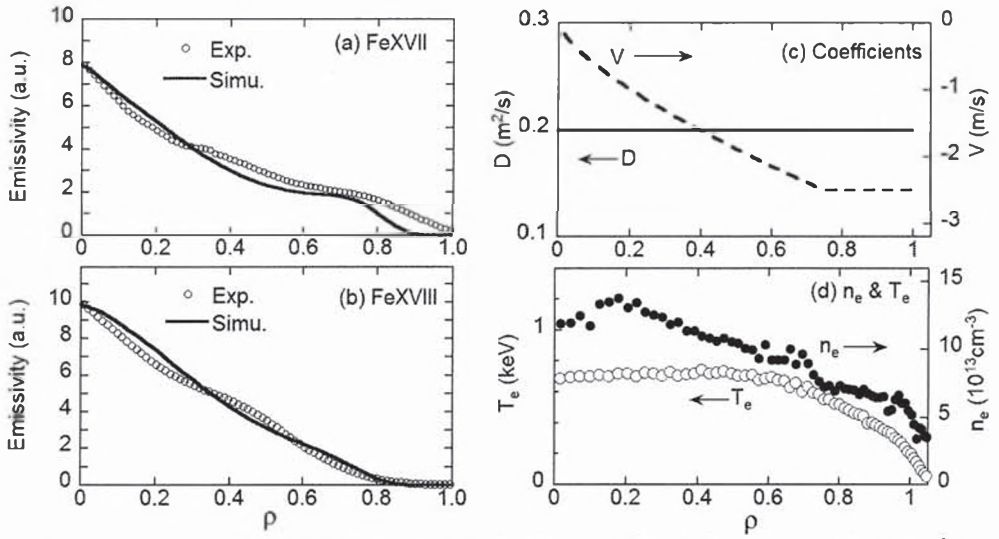

FIG. 5. Experimental (open circles) and simulated (solid line) profiles of (a) FeXVII at 15.02Å and (b) Fe XVIII at 14.20Å, (c) profiles of diffusion coefficient (solid line) and convective velocity (dashed line) and (d) profiles of electron temperature (open circles) and density (solid circles) .

Figure 6 shows the waveform of P_{NBI}, n_e, $T_e(0)$, P_{rad}, W_p and the intensity of the Fe Lα array in the wavelength range of 10-18Å. The emission profile is measured in the time frame denoted with hatched region in Fig. 6. The discharge is maintained at a relatively low density, $n_e < 5\times10^{13}cm^{-3}$. An iron pellet is injected at t = 3.8s for enhancing the iron emission. The intensity of Fe Lα emissions begins to decay just after the pellet injection, as seen in Fig. 6 (f). However, the intensity starts to increases at t = 4.2s after certain impurity confinement time. It strongly indicates iron ions accumulate into the plasma core.

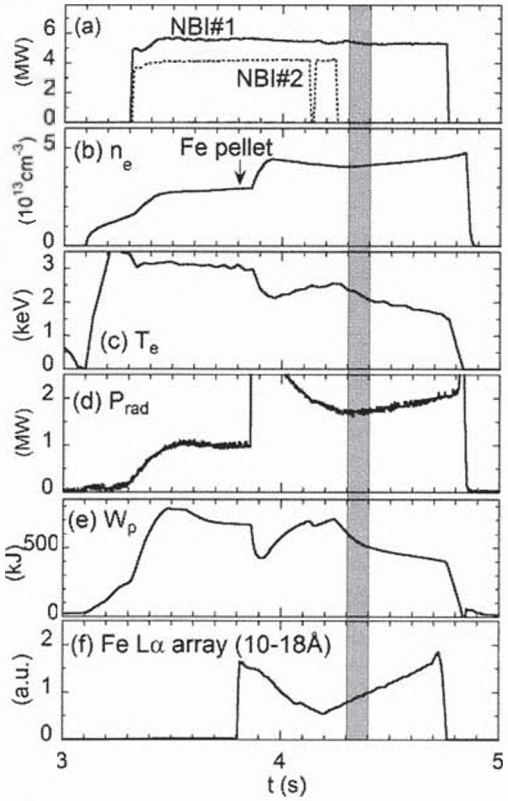

FIG. 6. Time evolution of (a) NBI port-through power, (b) line-averaged electron density, (c) central electron temperature, (d) plasma stored energy together, (e) radiation power and (f) total intensity of Fe Lα array located in the wavelength range 10-18Å.

Electron temperature and density profiles are shown in Fig. 7 (e). In contrast with high density case, the density profile exhibits a slightly hollow one with a central density of $4\times10^{13}cm^{-3}$. On the other hand, the electron temperature is much higher compared with the T_e profile in Fig. 5(e) and its profile shows a centrally peaked one. The emission profile of FeXVII at 15.02Å, Fe XX at 12.80-12.90Å and Fe XXIV at 10.62-10.66Å is plotted for both the measurement and simulation in Figs. 7 (a), (b) and (c), respectively. Reflecting the different ionization energy among three iron ions, each profile has its peak at different radial location. The transport code can well reproduce the profile if the transport coefficient has a radial structure shown in Fig. 7(d). Because of the uncertainty in the measurement and simulation, it is difficult to completely eliminate the deviation between the measurement and simulation in the profile fitting. Nevertheless, the radial structure of transport coefficients determined in the present study can give a valid information on the impurity transport in LHD. A weak outward convection, V = 0.5 m/s, is observed near the plasma center of $0.12 \leq \rho \leq 0.36$. This may be due to the positive gradient in the density profile. In the outer region of $0.36 \leq \rho \leq 1.0$, the convection is inversely changed and becomes inward. A detailed analysis on the radial structure of the convection velocity may require the information on the radial electric field, which sometimes plays an important role in the formation of impurity convection[13,14]. As for the diffusion coefficient, the D value of 0.06 m^2/s in the periphery region of $0.6 \leq \rho \leq 1.0$ is significantly lower than the value of 0.2 m^2/s seen in the plasma core. If the diffusion coefficient is assumed to be constant along the minor radius, the experimental profile cannot be entirely reproduced by the simulation code even if any combination is considered between the V and D. Therefore, the low D value appeared in the edge is justified by the present method using Lα transitions. Considering the collisionality of impurity ions[15], the reduction of D may be attributed to an increase in the collisionality because the iron ion stays in the $1/\nu$ or the plateau regime at the edge region.

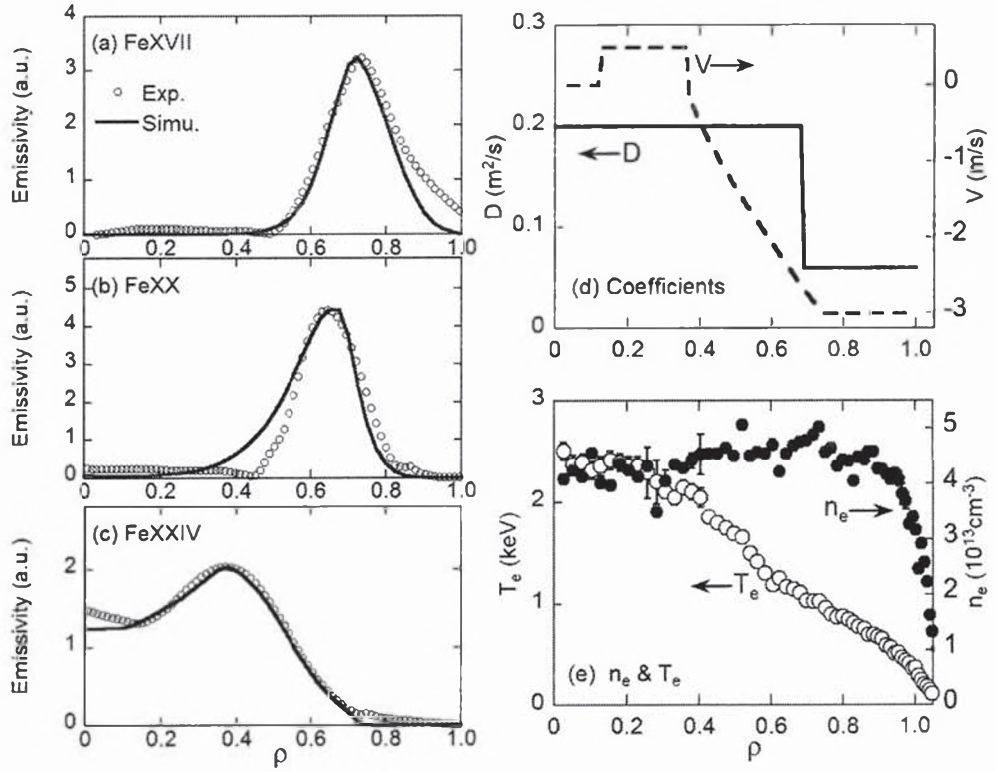

FIG. 7. Measured (open circles) and simulated (solid line) profiles of (a) FeXVII at 15.02Å, (b) FeXX at 12.80-12.90Å and (c) FeXXIV at 10.62-10.66Å, (d) profiles of diffusion coefficient (solid line) and convective velocity (dashed line) and (e) profiles of electron temperature (open circles) and density (solid circles) .

The convective velocity near ρ = 0.8 has been analyzed against the density gradient in low-density (n_e<5×10^{13}cm^{-3}) discharges using above-mentioned method. The result is plotted in Fig. 8. The convective velocity is proportional to the density gradient, which is similar to the conclusion of a previous study on C, Al and Ti[16]. In spite of this, more data are necessary to clarify the dependence of V on density gradient because the analyzed density range is limited in the present study.

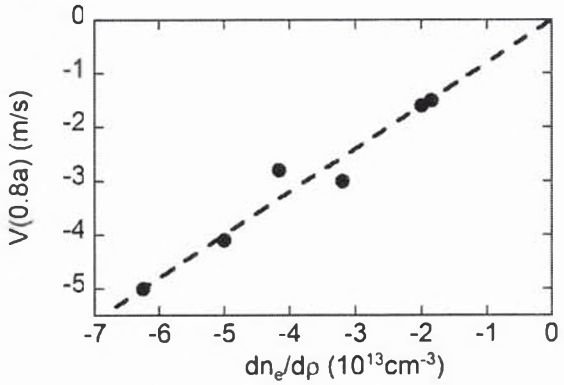

FIG. 8. Convective velocities as a function of density gradient near ρ=0.8 in low-density discharges (n_e<5×10^{13}cm^{-3}). Dashed line stands for linear fitting.

V. Summary

Using space-resolved EUV spectroscopy, we have studied the iron impurity transport under different conditions, such as n_e, R_{ax} and so on. With the help of one-dimensional impurity transport code, the transport coefficients of V and D are successfully obtained by analyzing the Fe Lα emission profile. Several discharges at low and high densities have been analyzed with the profile. One of the present results indicates that the inward convection determined at the plasma edge is proportional to the density gradient.

Acknowledgements

The authors thank all the members of the LHD experiment group for their cooperation including technical supports. This work was partly supported by the JSPS-NRF-NSFC A3 Foresight Program in the field of Plasma Physics (NSFC: No.11261140328, NRF : No. 2012K2A2A6000443).

References

[1]S. Morita, *et al.*, Plasma Sci. Technol. **8**, 55 (2006).
[2]M. Yoshinuma, *et al.*, Nucl. Fusion **49**, 062002 (2009).
[3]Y. Nakamura, *et al.*, Nucl. Fusion **43**, 219 (2003).
[4]Y. Igitkhanov, *et al.*, Plasma and Fusion Research **2**, S1131 (2007).
[5]C. F. Dong, *et al.*, Plasma Sci. Technol. **15**, 230 (2013).
[6]X. L. Huang, S. Morita, T. Oishi, M. Goto, and C. F. Dong, Rev. Sci. Instrum. **85**, 043511 (2014).
[7]R. Katai, S. Morita, M. Goto, H. Nishimura, K. Nagai, and S. Fujioka, Jpn. J. Appl. Phys. **46**, 3667 (2007).
[8]K. Yamazaki and L.E. Group, J. Plasma Fusion Res. **79**, 739 (2003).
[9]S. P. Hirshman, W.I. van RIJ, and P. Merkel, Computer Physics Communications **43**, 143 (1986).
[10]T. Amano, J. Mizuno, and J. Kako, Simulation of impurity transport in tokamak, Int. Rep. IPPJ-616, Institute of Plasma Physics, Nagoya University (1982).
[11]S. Morita, *et al.*, Plasma Sci. Technol. **8**, 55 (2006).
[12]A. Bar-Shalom, M. Klapisch, and J. Oreg, J. Quant. Spectrosc. Radiat. Trans., **71**, 169 (2001).
[13]K. Ida, *et al.*, Nucl. Fusion **45**, 391 (2005).
[14]Y. Igitkhanov, *et al.*, Plasma and Fusion Research **2**, S1131 (2007).
[15]S. Murakami, *et al.*, Nucl. Fusion **42**, L19 (2002).
[16]H. Nozato, *et al.*, Phys. Plasmas **13**, 092502 (2006).